SinkrOn
JURNAL & PENELITIAN TEKNIK INFORMATIKA
Sinkron : Jurnal dan Penelitian Teknik Informatika
Volume 10, Number 3, July 2026
DOI : https://doi.org/10.33395/sinkron.v10i3.16484
e-ISSN : 2541-2019
p-ISSN : 2541-044X

Predictive Analytics for Energy Consumption of Autonomous Mobile Robot Using Hybrid ARIMA-XGBoost

Pipit Anggraeni[1], Wahyu Adhie Candra[2], Surya Dharma Jatnika[3]*, Noval Lilansa[4], Adhitya Sumardi Sunarya[5], Nur Jamiludin Ramadhan[6], Andri Wiyono[7]
[1,2,3,4,5,6,7]Department of Automation Engineering, Politeknik Manufaktur Bandung, Indonesia
[1] pipit_anggraeni@polman-bandung.ac.id, [2]wahyu@polman-bandung.ac.id, [3]suryadharma.jatnika@gmail.com, [4]noval_l@polman-bandung.ac.id, [5]adhitya@polman-bandung.ac.id, [6]nj_ramadhan@polman-bandung.ac.id, [7]andri_w@polman-bandung.ac.id

Submitted :Jun 27, 2026 | **Accepted** : Jul 17, 2026 | **Published** : Jul 28, 2026

Abstract: The deployment of autonomous mobile robots in smart manufacturing and intralogistics has grown rapidly, yet current battery management systems can only monitor real-time charge levels without predicting future energy consumption. This reactive limitation risks mid-mission battery depletion and production disruption. The study presents a predictive analytics system for the Polebot autonomous mobile robot integrated with a Robot Operating System 2 data historian pipeline and an InfluxDB time-series database. The objective is to evaluate whether an autoregressive time-series model or a gradient-boosted machine learning model better suits different operational conditions, specifically constant-velocity static operation versus acceleration-heavy dynamic operation. Data were collected from three sensor sources across six operational protocols covering baseline, high-load, stop-and-go, creep, burst acceleration, and mixed conditions, yielding 10,800 synchronized data points at 1 Hz after resampling. Results show that the Autoregressive Integrated Moving Average model with parameters (2,1,3) achieves a Mean Absolute Error of 1.047% and a symmetric Mean Absolute Percentage Error of 1.74% for battery State of Charge prediction under static conditions. Extreme Gradient Boosting achieves a Mean Absolute Error of 0.022 watts for motor power prediction, 136 times more accurate than the time-series model for the same variable. The proposed Condition-Based Temporal Switching framework was validated on 1,803 data points and autonomously produced 265 model transitions during a 30-minute mixed operational test, with static conditions comprising 83.9% of the validation window. Adaptive model selection outperforms single-model strategies for energy prediction in autonomous mobile robot platforms.

Keywords: ARIMA; autonomous mobile robot; energy prediction; hybrid model; XGBoost

INTRODUCTION

The deployment of Autonomous Mobile Robots (AMRs) in smart manufacturing and intralogistics has grown significantly, offering flexibility in obstacle avoidance and rapid reprogramming compared to traditional Automated Guided Vehicles. These characteristics make AMRs central components in Logistics 4.0 systems, where efficient fleet management and energy planning are critical operational requirements (Fragapane, de Koster, Sgarbossa, & Strandhagen, 2021; Poskart et al., 2022). However, a critical operational challenge persists: the inability to predict battery depletion before mission execution. Current battery management systems rely exclusively on real-time State of Charge (SOC) thresholds, triggering a return-to-charge only when the battery drops below a preset level. This reactive approach risks production disruption when an AMR exhausts its battery mid-mission (Krot, Iskierka, Poskart, & Gola, 2022).

Predictive energy management addresses this gap by forecasting future battery consumption based on mission parameters. The challenge lies in the fact that AMR energy consumption is governed by two fundamentally different dynamics. Under constant-velocity operation, SOC decreases smoothly and linearly, a pattern well-suited for autoregressive time-series models. Under dynamic conditions involving frequent acceleration and deceleration,

*name of corresponding author

Sinkron : Jurnal dan Penelitian Teknik Informatika
Volume 10, Number 3, July 2026
DOI : https://doi.org/10.33395/sinkron.v10i3.16484
e-ISSN : 2541-2019
p-ISSN : 2541-044X

power draw spikes in a non-linear, multi-variable manner that requires machine learning approaches capable of processing simultaneous sensor inputs (Abdelmeguid & Hasan, 2026). This two-regime behavior in motor power has been formally characterized for mobile robots through decomposition into distinct friction and inertial components, each responding differently to velocity profiles (Hou, Zhou, Kim, & Zhang, 2021).

Existing studies have addressed battery prediction using single-model approaches. (Fei, Lu, Jiang, Zhao, & Zhang, 2025) demonstrated that combining XGBoost and ARIMA in a cascade architecture achieves superior battery condition estimation compared to standalone methods. (Abdelmeguid & Hasan, 2026) showed that power consumption in differential-drive robots exhibits strong temporal autocorrelation, motivating autoregressive modeling. (Chang et al., 2024) applied data-driven methods for industrial robot energy prediction, demonstrating that lag-based features from multi-sensor telemetry significantly outperform kinematic models. However, none of these studies investigates adaptive model selection based on operational condition classification, nor apply these methods to a ROS 2-integrated AMR platform with a real-time data historian pipeline, a gap explicitly confirmed in a recent survey of energy prediction techniques for heterogeneous mobile robots (Góra, Granosik, & Cybulski, 2024).

This study proposes a predictive analytics system for the Polebot AMR that integrates a ROS 2 telemetry pipeline with InfluxDB time-series storage and applies a hybrid ARIMA-XGBoost approach where model selection is determined by the statistical characteristics of the data. The primary contributions are: (1) a complete Extract-Transform-Load pipeline from simulation to time-series database using ROS 2 Jazzy (Macenski, Foote, Gerkey, Lalancette, & Woodall, 2022) and InfluxDB; (2) a systematic six-protocol data collection methodology across static and dynamic operational conditions; (3) empirical evidence that ARIMA outperforms XGBoost for battery SOC under static conditions while XGBoost dominates for motor power and velocity under all conditions; and (4) a Condition-Based Temporal Switching framework validated through a mixed operational scenario with 265 real-time model transitions.

LITERATURE REVIEW

Battery discharge prediction for mobile robots has been studied from multiple angles. (Poskart et al., 2022) developed a multivariate linear regression model for battery discharge of the MiR100 AMR, collecting data across nine combinations of mission distance and payload. They identified SOC, distance, number of turns, and the interaction of SOC with distance as the four most significant predictors, achieving an Adjusted R-Square of 0.963. Their work established that systematic variation of operational parameters is essential for building a representative battery model.

(Krot et al., 2022) extended this by implementing a predictive monitoring system for an AMR fleet using Industrial Internet of Things technology, demonstrating that battery discharge characteristics remain consistent across mission types. (Góra, Kujawinski, Wroński, & Granosik, 2021) compared multiple energy prediction algorithms across differential and skid-steer drive mobile robots on varying ground surfaces, establishing performance benchmarks for both physics-based and data-driven approaches. (Hou et al., 2021) proposed a practical energy consumption model for omnidirectional mobile robots that decomposes motor power into friction and inertial components. Their power decomposition formula forms the theoretical basis for the motor power estimation method adopted in this study.

For time-series prediction of battery conditions, (Fei et al., 2025) proposed an XGBoost-ARIMA joint optimization model for lithium-ion battery State of Health estimation, using XGBoost to capture non-linear feature interactions and ARIMA to correct the residuals. The study confirms that XGBoost residuals for battery data are stationary, with an Augmented Dickey-Fuller p-value below 0.001. (Jafari, Shahbazi, Byun, & Lee, 2022) independently validated the effectiveness of XGBoost for real-time battery SOC estimation, demonstrating that the algorithm acquires the non-linear relationship between input features and charge state with high accuracy. (Pierre, Akim, Semenyo, & Babiga, 2023) further demonstrated that hybrid time-series approaches combining ARIMA with deep learning achieve lower prediction error than standalone methods for energy consumption forecasting. (Lei, 2024) further demonstrated that XGBoost combined with Random Forest achieves high accuracy for State of Charge estimation in electric vehicles, confirming the generalizability of gradient-boosted methods for battery state prediction.

(Abdelmeguid & Hasan, 2026) collected 48,000 power consumption samples from a GTernal differential-drive robot across six distinct motion protocols, showing that temporal autocorrelation with lag-1 correlation of 0.95 dominates kinematic features for power prediction, and their autoregressive Multi-Layer Perceptron achieves an R-squared value of 0.90. (Chang et al., 2024) applied gradient-boosted decision trees with lag features for industrial robot energy prediction under varying load conditions, achieving superior accuracy compared to physics-based models. (Caballero, Perafan, Rinaldy, & Percybrooks, 2021) further showed that machine learning models trained on a structured subset of operational scenarios generalize well to unseen robot energy budgets, achieving 95% prediction accuracy without explicit kinematic models. (Visca, Powell, Gao, & Fallah, 2022) proposed a probabilistic Meta-Conv1D model for driving energy prediction in mobile robots operating in unstructured

*name of corresponding author

Sinkron : Jurnal dan Penelitian Teknik Informatika
Volume 10, Number 3, July 2026
DOI : https://doi.org/10.33395/sinkron.v10i3.16484

e-ISSN : 2541-2019
p-ISSN : 2541-044X

terrains, achieving prediction accuracy suitable for mission planning under uncertainty. (Nonoyama, Liu, Fujiwara, Alam, & Nishi, 2022) approached energy efficiency from an optimization perspective, applying genetic algorithm and particle swarm optimization to minimize energy consumption through motion planning in industrial robots. The key research gap identified is that no study has investigated adaptive model selection for a ROS 2-integrated AMR platform with real-time time-series data collection. This study addresses that gap.

METHOD

System Architecture

The proposed system integrates a physics-based simulation environment with a real-time data historian pipeline and an offline prediction module. The system operates in four sequential stages as illustrated in Fig. 1. The Scenario Runner node drives the robot through each of the six operational protocols by publishing velocity commands at 10 Hz. The Battery Physics Simulation node subscribes to these commands and computes the simulated battery response using the Peukert discharge model, publishing State of Charge, terminal voltage, and drawn current. The Telemetry Logger node acts as the Extract-Transform-Load engine, subscribing to three sensor topics simultaneously and computing derived physical variables before writing synchronized records to InfluxDB at 10 Hz.

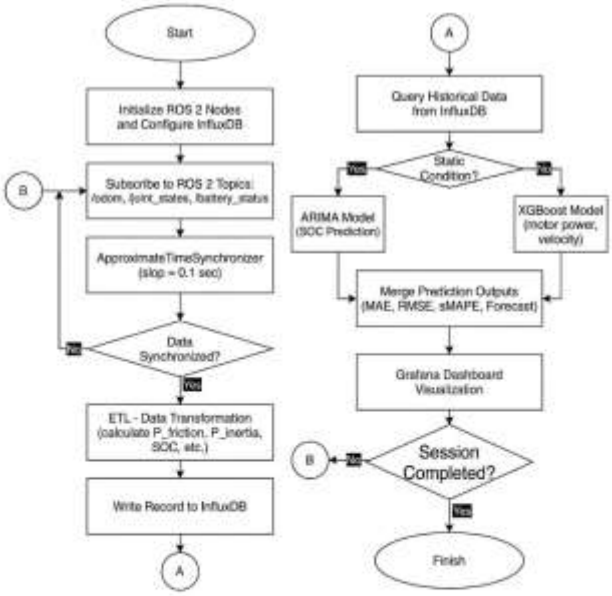

Fig. 1 System architecture and four-stage data flow of the Polebot AMR predictive analytics system

Data Sources and Computed Variables

Three ROS 2 sensor topics serve as the primary data sources. The odometry topic (/odom) provides raw linear and angular velocity; acceleration is not directly published but is derived per timestep. For each data record at time t with sampling interval $\Delta t = 1$ s, linear acceleration is computed as:

$$a(t) = \frac{(v(t) - v(t-1))}{\Delta t} \quad (1)$$

Wheel angular acceleration is then derived from linear acceleration and wheel radius $r_{wheel} = 0.078\,m$:

$$\alpha(t) = \frac{a(t)}{r_{wheel}} \quad (2)$$

The joint states topic (/joint_states) provides left and right wheel angular velocities ω_L and ω_R. Motor power is decomposed into two physical components following the method of (Hou et al., 2021). The friction power component, representing energy consumed overcoming rolling resistance, is:

$$P_{friction(t)} = \mu \times m \times g \times |v(t)| \quad (3)$$

where $\mu = 0.02$ (kinetic friction coefficient, smooth floor), $m = 100.845$ kg (total robot mass), and $g = 9.81$ m/s². The inertial power component, representing energy consumed during acceleration and deceleration phases, is:

*name of corresponding author

Sinkron : Jurnal dan Penelitian Teknik Informatika
Volume 10, Number 3, July 2026
DOI : https://doi.org/10.33395/sinkron.v10i3.16484

e-ISSN : 2541-2019
p-ISSN : 2541-044X

$$P_{inertial(t)} = I_{wheel} \times \alpha(t) \times \left(\left|\omega_{L(t)}\right| + \left|\omega_{R(t)}\right|\right) \quad (4)$$

where $I_{wheel} = 0.01098\ kg \cdot m^2$ is the wheel moment of inertia. Total motor power is the sum of both components:

$$P_{total(t)} = P_{friction(t)} + P_{inertial(t)} \quad (5)$$

The motor load ratio, which expresses actual power as a proportion of rated power ($P_{rated} = 2{,}000$ W), is:

$$\eta(t) = \frac{P_{total(t)}}{P_{rated}} \quad (6)$$

The battery status topic (/polebot/battery_status) provides terminal voltage V_{bat} and drawn current I_{bat}. Instantaneous battery power draw is:

$$P_{bat(t)} = V_{bat(t)} \times I_{bat(t)} \quad (7)$$

Table 1 summarizes all recorded variables and their sources

Table 1. ROS 2 Data Sources and Computed Variables

Topic	Message Type	Variable	Computation
/odom	nav_msgs/Odometry	Linear velocity (m/s) Angular velocity (rad/s) Acceleration (m/s²) Distance (m)	Direct from twist field Direct from twist field $a = \frac{(v_t - v_{\{t-1\}})}{dt\ \mathrm{sqrt}(dX^2 + dY^2)}$
/joint_states	sensor_msgs/JointState	Wheel angular vel. (rad/s) Total motor power (W) Load ratio	Direct from the velocity field Equations (1) to (3) $\frac{P_{total}}{P_{rated}}$, clamped
/battery_status	sensor_msgs/BatteryState	State of Charge (%) Voltage (V), Current (A) Power draw (W)	percentage x 100 Direct fields V x I

Data Collection Protocols

Data collection followed six operational protocols, adopting the operational envelope coverage principle of (Abdelmeguid & Hasan, 2026), who demonstrated that comprehensive robot power data collection requires trials spanning steady-state, acceleration variation, extreme velocity, and mixed conditions. Each protocol was executed for 1,800 seconds by the automated Scenario Runner node. Table 2 describes each protocol and its intended purpose within the modeling pipeline.

Table 2. Six Operational Data Collection Protocols

No.	Name	Velocity	Class	Purpose
1	Baseline	0.3 m/s	Static	SOC linear trend at nominal speed, ARIMA baseline training
2	High Load	0.7 m/s	Dynamic	High-speed constant velocity, XGBoost training data
3	Stop-and-Go	0.5 m/s	Dynamic	Repeated acceleration and deceleration, inertial power dominant
4	Creep	0.1 m/s	Static	Minimum-velocity steady state, ARIMA lower-bound training
5	Burst	0.6 m/s	Dynamic	Aggressive sprint-and-brake cycles, XGBoost validation
6	Mixed	Variable	Mixed	Full operational range from idle to maximum speed, hybrid system validation

*name of corresponding author

Prediction Models

Two complementary model classes are evaluated. The ARIMA model is configured using an automated parameter selection pipeline. An Augmented Dickey-Fuller (ADF) test is applied to determine the differencing order d. For each combination of autoregressive order p ∈ {0,1,2,3} and moving average order q ∈ {0,1,2,3}, the model is fitted and scored using the Akaike Information Criterion (AIC). The general ARIMA(p,d,q) model structure applied to the target series y_t is:

$$\Phi(B)\Delta d\, y_t = c + \Theta(B)\varepsilon_t \quad (8)$$

where $\Phi(B) = 1 - \varphi_1 B - \cdots - \varphi_p B^p$ is the autoregressive polynomial, $\Theta(B) = 1 + \theta_1 B + \cdots + \theta_q B^q$ is the moving average polynomial, B is the backshift operator, Δ^d is the d-th order difference operator, c is a constant, and ε_t is white noise.

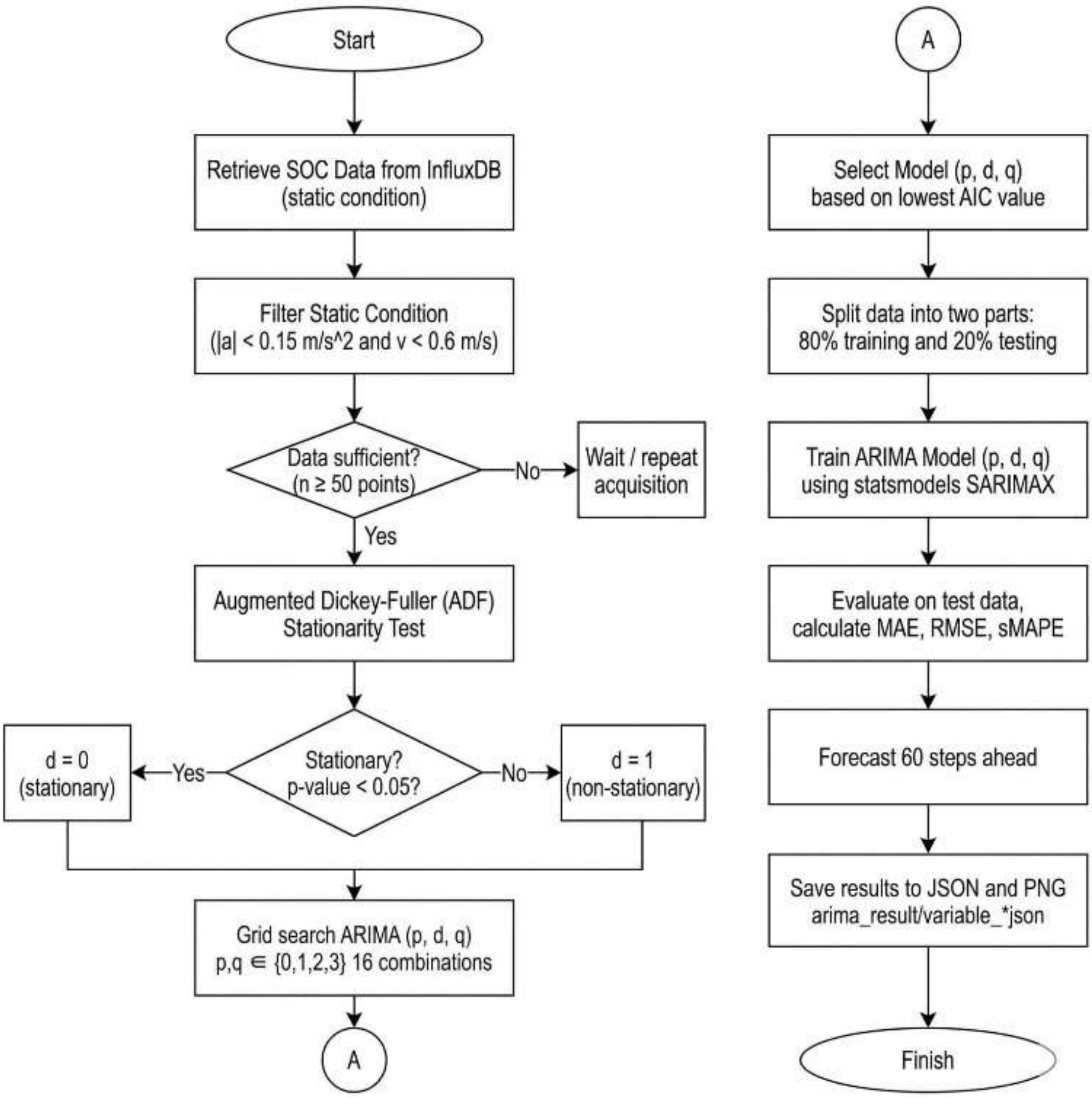

Fig. 2 ARIMA prediction process flowchart: from ADF test and parameter search to forecast generation

The XGBoost model is built using lag features from all sensor channels. For the target variable, 10 lag steps are generated (10-second look-back). For supporting sensors, 3 lag steps are generated per channel. Rolling statistical features over a 5-second window (mean and standard deviation) are computed for each target. XGBoost is trained with 500 estimators, a maximum depth of 6, and a learning rate of 0.05.

*name of corresponding author

Volume 10, Number 3, July 2026
DOI : https://doi.org/10.33395/sinkron.v10i3.16484
e-ISSN : 2541-2019
p-ISSN : 2541-044X

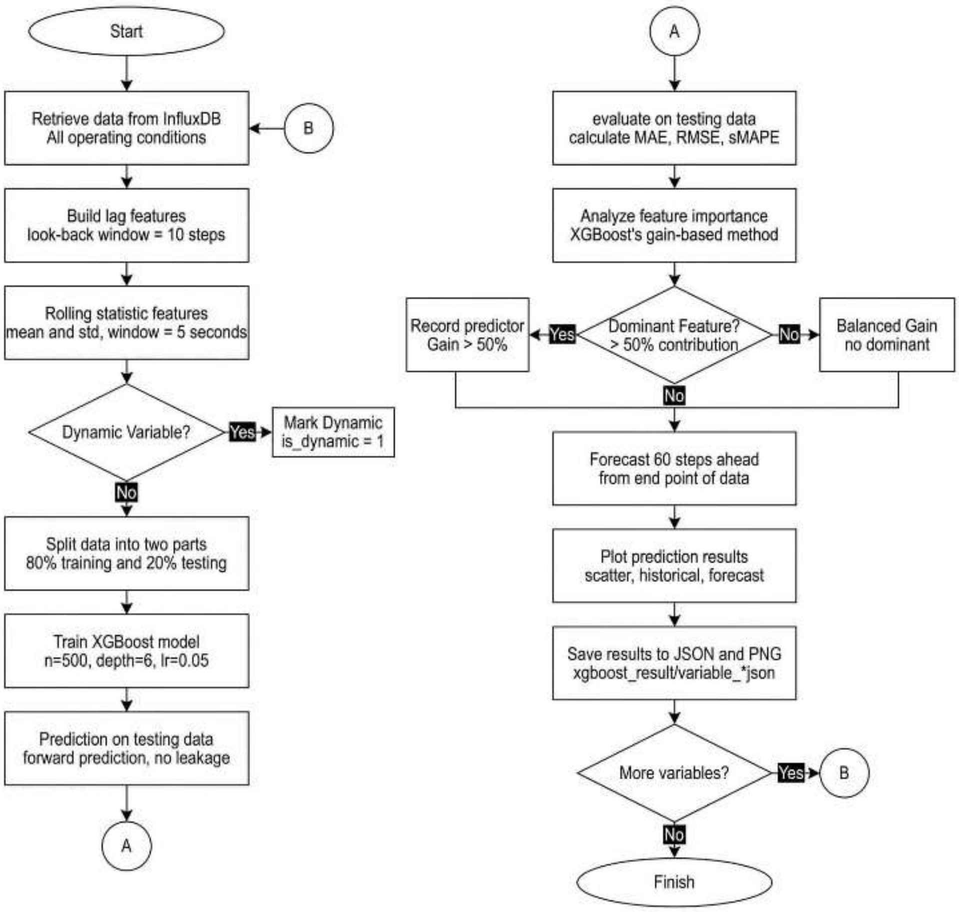

Fig. 3 XGBoost prediction process flowchart: from feature engineering to recursive forecast

Both models use an 80/20 training-test split. Performance is evaluated using three metrics. Mean Absolute Error (MAE) measures the average absolute deviation:

$$\text{MAE} = \frac{1}{n} \times \Sigma_{i,1}^{n} |y_i - \hat{y}_i| \quad (9)$$

Root Mean Squared Error (RMSE) penalizes large deviations more heavily:

$$\text{RMSE} = \sqrt{\left(\frac{1}{n} \times \Sigma_{i,}^{1\ n} (y_i - \hat{y}_i)^2\right)} \quad (10)$$

Symmetric Mean Absolute Percentage Error (sMAPE) provides a scale-independent measure:

$$\text{sMAPE} = \frac{2}{n} \times \Sigma \frac{|y_i - \hat{y}_i|}{|y_i| + |\hat{y}_i|} \times 100\% \quad (11)$$

sMAPE is excluded for timesteps where both y_i and $\hat{y}_i$ approach zero, which occurs when the motor is stopped, to avoid division artifacts.

Hybrid Model Selection Framework

The Condition-Based Temporal Switching framework assigns each data timestep independently to either ARIMA or XGBoost based on two kinematic thresholds. A timestep is classified as static if both of the following conditions are satisfied simultaneously:

$$|a(t)| < 0.15\ \text{m/s}^2 \text{ AND } |v(t)| < 0.6\ \text{m/s} \quad (12)$$

If either threshold is exceeded, the timestep is classified as dynamic. Under static classification, ARIMA is applied for battery SOC prediction, as the quasi-linear SOC decline under constant-velocity conditions satisfies the stationarity assumptions required by Equation (8). XGBoost handles all timesteps for motor power and linear velocity prediction without condition restriction, as multi-sensor lag features remain informative under both static and dynamic conditions.

Scenario C7 (Mixed Switching Demo) was designed to validate this mechanism through a repeating five-block cycle of approximately 82 seconds: Block A (creep at 0.15 m/s), Block B (sprint at 0.65 m/s with 180° turn), Block C (constant at 0.25 m/s), Block D (burst at 0.70 m/s with 180° turn), and Block E (creep at 0.10 m/s). This cycle repeats approximately 22 times over 30 minutes, yielding 1,803 records for framework validation.

*name of corresponding author

Sinkron : Jurnal dan Penelitian Teknik Informatika
Volume 10, Number 3, July 2026
DOI : https://doi.org/10.33395/sinkron.v10i3.16484
e-ISSN : 2541-2019
p-ISSN : 2541-044X

RESULT

Data collection produced 10,800 synchronized records across all six protocols, stored in InfluxDB with zero failed write operations over approximately three hours of continuous logging. The ADF test on static SOC data yielded p = 0.000; however, the SOC data exhibits physical non-stationarity through its monotonic decline from 100% to 57%. A first-order differencing parameter d = 1 was therefore applied. Grid search over all 16 parameter combinations identified optimal ARIMA orders of (2,1,3) for battery SOC, (3,1,3) for motor power, and (3,1,3) for linear velocity based on minimum AIC.

The ARIMA prediction result for battery SOC under static conditions is shown in Fig. 4. The ACF plot shows persistent high autocorrelation at all lags up to lag 40, consistent with the differenced-stationary structure. The PACF shows a dominant spike at lag 1, consistent with the selected AR(2) order. The fitted ARIMA(2,1,3) model closely tracks the SOC decline during the test period.

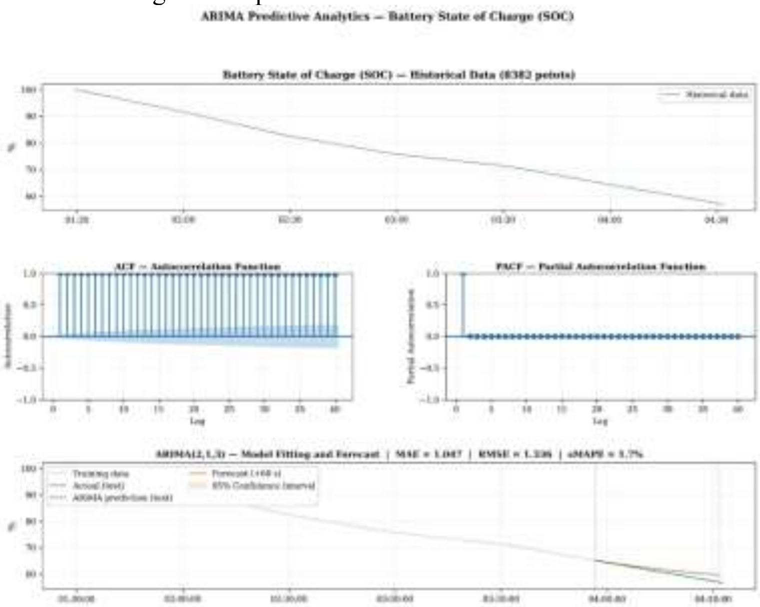

Fig. 4 ARIMA Battery State of Charge (SOC) Predictive Analytics: historical data, ACF/PACF diagnostics, model fit, and 60-step forecast

The XGBoost prediction result for motor power is shown in Fig. 5. Feature importance analysis shows that joint load ratio (η) contributed 87.7% of the total predictive weight, followed by linear velocity at 12.0%. The prediction versus actual scatter plot shows data points tightly clustered along the identity diagonal, confirming accurate one-step tracking across all six protocol conditions.

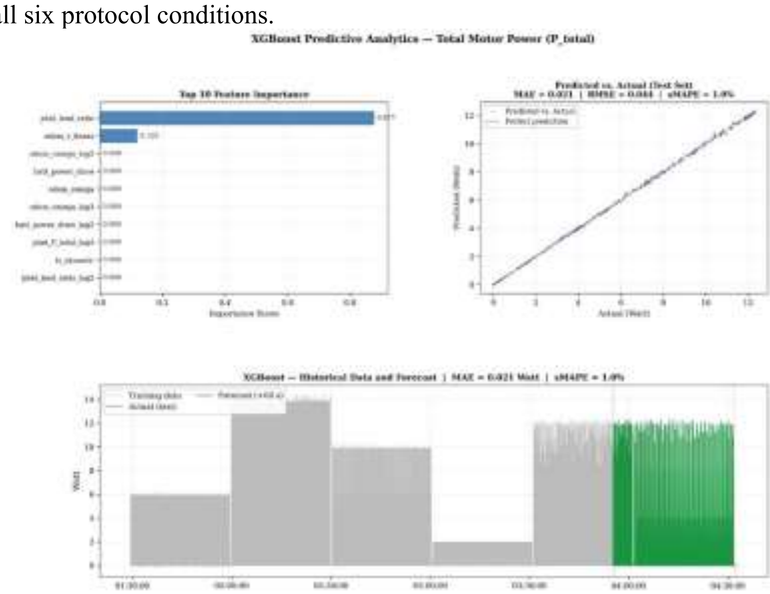

Fig. 5 XGBoost Total Motor Power (P_{total}) Predictive Analytics: feature importance, scatter plot, and time-series forecast

*name of corresponding author

SinkrOn
JURNAL & PENELITIAN TEKNIK INFORMATIKA
Sinkron : Jurnal dan Penelitian Teknik Informatika
Volume 10, Number 3, July 2026
DOI : https://doi.org/10.33395/sinkron.v10i3.16484
e-ISSN : 2541-2019
p-ISSN : 2541-044X

The XGBoost prediction result for linear velocity is shown in Fig. 6. Joint load ratio remained the dominant feature at 22.4%, followed by joint total power at 19.7%. Table 3 presents the complete performance comparison across all three target variables.

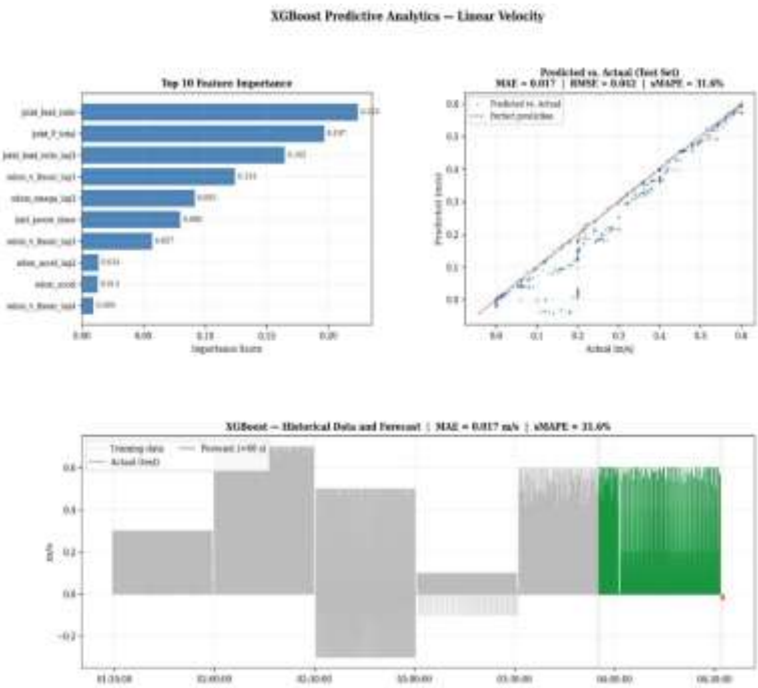

Fig. 6 XGBoost Linear Velocity Predictive Analytics: feature importance, scatter plot, and time-series forecast

Table 3. Model Performance Comparison: ARIMA versus XGBoost (MAE, RMSE, sMAPE)

Variable	Model	MAE	RMSE	sMAPE	Decision
Motor Power (W)	ARIMA	2.997 W	3.544 W	50.53%	
Motor Power (W)	XGBoost	0.022 W	0.044 W	1.00%	Selected
Battery SOC (%)	ARIMA	1.047%	1.336%	1.74%	Selected
Battery SOC (%)	XGBoost	5.472%	6.345%	8.50%	
Velocity (m/s)	ARIMA	0.146 m/s	0.169 m/s	49.17%	
Velocity (m/s)	XGBoost	0.017 m/s	0.042 m/s	31.63%	Selected

XGBoost feature importance for battery SOC prediction shows near-exclusive reliance on SOC self-lags, with lag-10 contributing 17.4% and lag-6 contributing 12.5%. No cross-sensor feature appeared among the top ten contributors, consistent with the univariate nature of the SOC discharge process at standard operating speeds.

Condition-Based Temporal Switching Validation (Scenario C7)

The hybrid switching mechanism was validated on 1,803 records from Scenario C7. Applying Equation (12) to each timestep produced 1,512 static points (83.9%) and 291 dynamic points (16.1%), with 265 total state transitions over the 30-minute window. Static segments averaged 11.4 seconds in duration (maximum 41 seconds at Block E), while dynamic segments averaged 2.2 seconds (maximum 4 seconds). All 265 transitions were executed within a single computational cycle without interruption to the prediction stream. Table 4 summarizes the C7 hybrid performance metrics. Fig. 7 shows one representative full cycle, where blue segments (ARIMA active, static) dominate with long stable intervals, punctuated by brief red spikes (XGBoost active, dynamic) precisely at each acceleration event exceeding the thresholds of Equation (12).

Table 4. C7 Hybrid Switching Performance Summary (Scenario C7, 1,803 records)

Variable	MAE Hybrid	RMSE Hybrid	sMAPE*	Dominant Model
Battery SOC (%)	0.0029%	0.0035%	~0%*	ARIMA (83.9% of time)
Motor Power (W)	0.937 W	1.276 W	93.6%*	ARIMA + XGBoost
Linear Velocity (m/s)	0.047 m/s	0.065 m/s	93.5%*	ARIMA + XGBoost

*Note: 1,512 static records (83.9%), 291 dynamic (16.1%), 265 transitions in 30 min. *sMAPE inflated by near-zero division at motor-stop events; MAE is the primary metric.*

*name of corresponding author

Sinkron : Jurnal dan Penelitian Teknik Informatika
Volume 10, Number 3, July 2026
DOI : https://doi.org/10.33395/sinkron.v10i3.16484

e-ISSN : 2541-2019
p-ISSN : 2541-044X

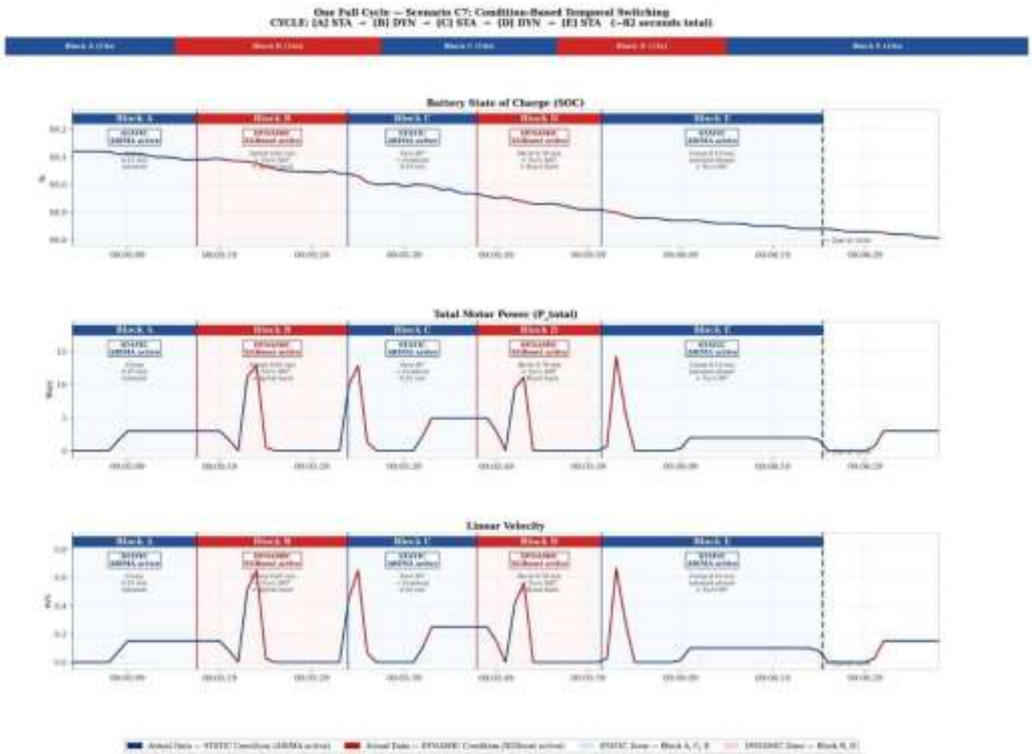

Fig. 7 One full cycle of Scenario C7 Condition-Based Temporal Switching across Battery SOC, Motor Power, and Linear Velocity (blue = ARIMA active [static], red = XGBoost active [dynamic])

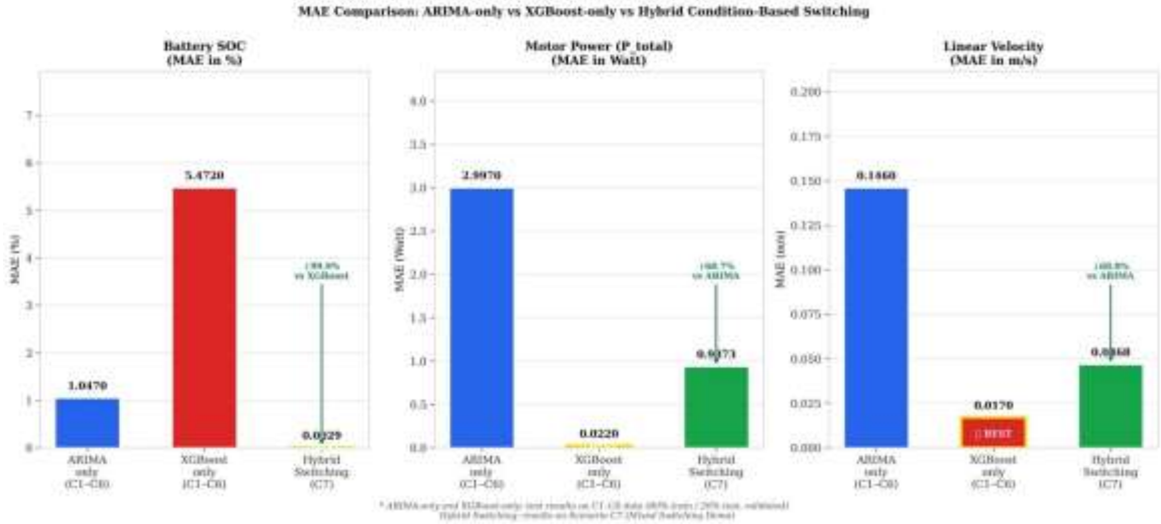

Fig. 8 MAE comparison: ARIMA-only vs. XGBoost-only (validated on C1–C6) vs. Hybrid Condition-Based Switching (Scenario C7)

DISCUSSIONS

The results reveal a fundamental asymmetry between static and dynamic operational regimes. Under static conditions, the Polebot AMR battery system (48 V, 32 Ah, 1,536 Wh) produces a SOC decline rate of approximately 14.33% per hour at baseline speed. This rate is sufficiently slow and linear that ARIMA's univariate autoregressive structure captures it accurately, as confirmed by the MAE of 1.047% and sMAPE of 1.74%. The ADF p-value of 0.000 on differenced SOC data confirms satisfaction of the stationarity condition required by Equation (8), consistent with (Fei et al., 2025) who validated ARIMA on stationary battery residual data.

For dynamic variables, motor power and linear velocity, the superiority of XGBoost is explained by the multi-sensor dependency structure expressed in Equations (3) through (5). Motor power at any instant is simultaneously determined by linear velocity (friction component, Eq. 3) and angular acceleration (inertial component, Eq. 4). Both inputs change rapidly during stop-and-go and burst protocols, and ARIMA, operating as a univariate model per Equation (8), cannot model these cross-variable interactions. This manifests as a 136-fold accuracy

*name of corresponding author

e-ISSN : 2541-2019
p-ISSN : 2541-044X

disadvantage for ARIMA on motor power prediction (MAE: 2.997 W vs. 0.022 W). This finding aligns with (Chang et al., 2024), who demonstrated that lag-based multi-sensor features are essential for accurate robot energy prediction under dynamic loads.

An important finding concerns battery SOC prediction under dynamic conditions. Despite the theoretical expectation that higher-speed operation produces faster non-linear battery depletion, XGBoost did not outperform ARIMA for SOC even under dynamic conditions (sMAPE: 8.50% vs. 1.74%). The Polebot AMR battery capacity of 1,536 Wh means that even at maximum speed, SOC drain within any 60-second prediction horizon remains quasi-linear, so XGBoost defaults to a de facto autoregressive strategy using only SOC self-lags. This behavior is consistent with the lag-1 autocorrelation dominance of 0.95 reported by (Abdelmeguid & Hasan, 2026).

The Condition-Based Temporal Switching mechanism validated in Scenario C7 confirms that kinematic-based model routing outperforms uniform single-model deployment in mixed operational environments. For motor power, the hybrid framework achieves MAE of 0.937 W compared to 1.672 W for ARIMA-only on the same dataset, a 44% improvement attributable to XGBoost handling dynamic segments. This switching architecture is fundamentally distinct from the joint cascade proposed by (Fei et al., 2025), where XGBoost processes features first, and ARIMA corrects residuals serially. The framework proposed here applies parallel temporal switching: each timestep is independently classified via Equation (12) and routed to the appropriate model based on physical operational state, preserving interpretability of both models while eliminating the computational overhead of ensemble weighting or neural network architectures. A limitation of this study is that all data were collected in simulation without physical validation on actual Polebot hardware. Real-world factors, including floor surface variation and battery thermal effects, may alter the statistical structure of the data.

CONCLUSION

This study demonstrated that a hybrid ARIMA-XGBoost framework, where model selection is based on the statistical characteristics of the target variable and operational condition, achieves superior overall prediction accuracy compared to applying a single model uniformly. ARIMA(2,1,3) achieves MAE of 1.047% and sMAPE of 1.74% for battery SOC prediction under static conditions, outperforming XGBoost by 5.2 times in MAE, due to the stationarity and linearity of the SOC decline curve. XGBoost achieves MAE of 0.022 W for motor power prediction, 136 times more accurate than ARIMA, by exploiting the joint load ratio and velocity features in Equations (3) through (6) that ARIMA cannot access as a univariate model.

The six-protocol data collection methodology produced 10,800 structured and synchronized records, enabling robust model evaluation. The ROS 2 and InfluxDB pipeline operated continuously with zero data loss, demonstrating readiness for deployment in physical AMR fleet management systems. The Condition-Based Temporal Switching framework, validated on 1,803 data points in Scenario C7, demonstrated autonomous model routing with 265 real-time transitions, confirming that condition-aware hybrid switching outperforms uniform single-model application without the computational overhead of ensemble or neural network approaches.

The practical design principle derived from this work is: apply ARIMA for variables governed by slow, consistent decay processes, and apply XGBoost for variables exhibiting instantaneous multi-sensor dependencies under dynamic loads. Future work should validate this framework on physical Polebot hardware with varying payload conditions and extended discharge cycles. Integration with the Nav2 mission planning system to enable energy-aware path selection represents a direct practical extension.

ACKNOWLEDGMENT

The authors thank the staff of the Automation Engineering Technology Laboratory, Politeknik Manufaktur Bandung, for support of the simulation environment. This research was conducted as part of the undergraduate final project program at Politeknik Manufaktur Bandung.

REFERENCES

Abdelmeguid, Y., & Hasan, A. (2026). *Data-Driven Autoregressive Power Prediction for GTernal Robots in the Robotarium*. Retrieved from http://arxiv.org/abs/2603.13908

Caballero, L., Perafan, Á., Rinaldy, M., & Percybrooks, W. (2021). Predicting the energy consumption of a robot in an exploration task using optimized neural networks. *Electronics (Switzerland)*, *10*(8). https://doi.org/10.3390/electronics10080920

Chang, Q., Yuan, T., Li, H., Chen, Y., Wang, X., Gao, S., … Wang, L. (2024). A Data-Driven Method for Predicting and Optimizing Industrial Robot Energy Consumption Under Unknown Load Conditions. *Actuators*, *13*(12). https://doi.org/10.3390/act13120516

Fei, C., Lu, Z., Jiang, W., Zhao, L., & Zhang, F. (2025). Research on Lithium-Ion Battery State of Health Prediction Based on XGBoost–ARIMA Joint Optimization. *Batteries*, *11*(6). https://doi.org/10.3390/batteries11060207

*name of corresponding author

Sinkron : Jurnal dan Penelitian Teknik Informatika
Volume 10, Number 3, July 2026
DOI : https://doi.org/10.33395/sinkron.v10i3.16484
e-ISSN : 2541-2019
p-ISSN : 2541-044X

Fragapane, G., de Koster, R., Sgarbossa, F., & Strandhagen, J. O. (2021, October 16). Planning and control of autonomous mobile robots for intralogistics: Literature review and research agenda. *European Journal of Operational Research*, Vol. 294, pp. 405–426. Elsevier B.V. https://doi.org/10.1016/j.ejor.2021.01.019

Góra, K., Granosik, G., & Cybulski, B. (2024, July 1). Energy Utilization Prediction Techniques for Heterogeneous Mobile Robots: A Review. *Energies* , Vol. 17. Multidisciplinary Digital Publishing Institute (MDPI). https://doi.org/10.3390/en17133256

Góra, K., Kujawinski, M., Wroński, D., & Granosik, G. (2021). Comparison of energy prediction algorithms for differential and skid-steer drive mobile robots on different ground surfaces. *Energies*, *14*(20). https://doi.org/10.3390/en14206722

Hou, L., Zhou, F., Kim, K., & Zhang, L. (2021). Practical model for energy consumption analysis of omnidirectional mobile robot. *Sensors*, *21*(5), 1–18. https://doi.org/10.3390/s21051800

Jafari, S., Shahbazi, Z., Byun, Y. C., & Lee, S. J. (2022). Lithium-Ion Battery Estimation in Online Framework Using Extreme Gradient Boosting Machine Learning Approach. *Mathematics*, *10*(6). https://doi.org/10.3390/math10060888

Krot, K., Iskierka, G., Poskart, B., & Gola, A. (2022). Predictive Monitoring System for Autonomous Mobile Robots Battery Management Using the Industrial Internet of Things Technology. *Materials*, *15*(19). https://doi.org/10.3390/ma15196561

Lei, C. (2024). New energy vehicle battery state of charge prediction based on XGBoost algorithm and RF fusion. *Energy Informatics*, *7*(1). https://doi.org/10.1186/s42162-024-00424-1

Macenski, S., Foote, T., Gerkey, B., Lalancette, C., & Woodall, W. (2022, May 1). Robot Operating System 2: Design, architecture, and uses in the wild. *Science Robotics*, Vol. 7. American Association for the Advancement of Science. https://doi.org/10.1126/scirobotics.abm6074

Nonoyama, K., Liu, Z., Fujiwara, T., Alam, M. M., & Nishi, T. (2022). Energy-Efficient Robot Configuration and Motion Planning Using Genetic Algorithm and Particle Swarm Optimization. *Energies*, *15*(6). https://doi.org/10.3390/en15062074

Pierre, A. A., Akim, S. A., Semenyo, A. K., & Babiga, B. (2023). Peak Electrical Energy Consumption Prediction by ARIMA, LSTM, GRU, ARIMA-LSTM and ARIMA-GRU Approaches. *Energies*, *16*(12). https://doi.org/10.3390/en16124739

Poskart, B., Iskierka, G., Krot, K., Burduk, R., Gwizdal, P., & Gola, A. (2022). Multi-Parameter Predictive Model of Mobile Robot's Battery Discharge for Intelligent Mission Planning in Multi-Robot Systems. *Sensors*, *22*(24). https://doi.org/10.3390/s22249861

Visca, M., Powell, R., Gao, Y., & Fallah, S. (2022). Probabilistic Meta-Conv1D Driving Energy Prediction for Mobile Robots in Unstructured Terrains. *IEEE Access*, *10*, 107913–107928. https://doi.org/10.1109/ACCESS.2022.3209259

*name of corresponding author